A multisource transportation network model explaining allometric scaling

Jia, Xiang Yu; Liu, Er Jian; Yang, Yitao; Yan, Xiao Yong

Important note
To cite this publication, please use the final published version (if applicable).
Please check the document version above.

PAPER

A multisource transportation network model explaining allometric scaling

View the article online for updates and enhancements.

A multisource transportation network model explaining allometric scaling

Xiang-Yu Jia[1]**, Er-Jian Liu**[1,2,*]**, Yitao Yang**[1,3]
and Xiao-Yong Yan[1]

[1] School of Systems Science, Beijing Jiaotong University, Beijing 100044, People's Republic of China
[2] Instituto de Física Interdisciplinar y Sistemas Complejos IFISC (CSIC-UIB), Palma de Mallorca 07122, Spain
[3] Department of Transport & Planning, Faculty of Civil Engineering and Geosciences, Delft University of Technology, Stevinweg1, Delft 2628 CN, The Netherlands
E-mail: erjianliu@bjtu.edu.cn

Abstract. The universal scaling relationship between an attribute and the size of a system is widespread in nature and society and is known as allometric growth. Previous studies have explained that the allometric growth exponent of single-source systems is uniquely determined by the dimension. However, the phenomenon that the exponent shows diversity in some systems, such as rivers, freight transportation and gasoline stations, lacks a reasonable explanation. In this paper, we hold the view that allometric growth may originate from efficient delivery from sources to transfer sites in a system and propose a multisource transportation network model that can explain diversified allometric growth exponents. We apply this model to some multisource systems, and the results show that our model successfully reproduces the diversity of the allometric growth exponent.

*Author to whom any correspondence should be addressed.

Contents

1. Introduction

Allometric growth is an important research topic in many disciplines ranging from biology to urban science. It is the scaling relationship between a system attribute (e.g. an organism's metabolic rate, lifespan, urban road area) and the size of the system (e.g. an organism's weight or volume, the population of a city). The law of allometric growth was originally discovered by biologists [1–5], which states that the basal metabolic rate level of animals (including mammals, reptiles, insects) is proportional to the 3/4 power of their three-dimensional body mass. In addition, there are also numerous two-dimensional systems and even one-dimensional systems that exhibit allometric growth. For instance, Olaf Dreyer used a one-dimensional experiment to discover that the length and mass of water flowing in a single direction on a permeable tissue showed an allometric growth relationship with an exponent of 1/2 [6]. Banavar discovered that the relationship between the flow and size of each tributary for a two-dimensional river system can be expressed by an allometric growth equation with an exponent of 2/3 [7]. Significant allometric growth has also been observed in two-dimensional urban systems, but the allometric growth exponent is diversified and no longer 2/3 [8–12]. For example, the growth of urban infrastructure (e.g. cable length [13], road area [14], number of gasoline stations [15]) tends to be sublinear compared to the size of the city (expressed in terms of population), with an allometric growth exponent between 2/3 and 1. On the other hand, the growth of wealth creation and innovation in cities (e.g. GDP [16],

number of new patents [17] and inventions [18]) tends to be superlinear compared to city size, with an allometric growth exponent greater than 1. Furthermore, Rocha *et al* found that the number of social interactions in animal groups, including humans and other mammals, also exhibit a superlinear allometric growth relationship with group size [19].

More recently, researchers have focused on providing a reasonable explanation for allometric growth scaling and revealing the nature of allometric growth. West *et al* proposed a model that established the mechanism of energy and material transfer from an organism to terminals through a branching tube network to explain allometric growth from a fractal perspective [2, 20]. It can explain the allometric growth exponent $D/(D+1)$ of living organisms, where D is the dimension, but lacks an explanation for nonliving organisms [21]. Banavar *et al* proposed a single-source transportation network (STN) model [7]. A transportation network is a flow network with one source or multiple sources where the flow originates or converges. For example, in the cardiovascular system, nutrients originate from a single source (the heart), and flow to various organs. Hence, the cardiovascular system qualifies as a single-source transportation network. In the urban gasoline station system, multiple gasoline stations serve customers across the city, making the gasoline station system a multisource transportation network. The STN model clearly illustrates how network topology can affect resource transport efficiency and how the most effective structure can introduce the $D/(D+1)$ power exponential form [7]. It is successful in explaining the allometric growth of not only living organisms but also rivers. However, it cannot explain the diversified allometric growth exponents (not always 2/3) presented in urban systems. This is primarily caused by the fact that most urban resource transportation networks have multiple sources [22, 23]. Unlike the STN model, Samaniego and Moses developed a fully decentralized transportation network (DTN) model by assuming that people would travel to each nearby location that can be considered a source [24]. The DTN and STN models are the two extreme scenarios for transportation networks. Many transportation networks, both in natural and social systems, are multisource networks rather than single-central or fully decentralized networks. However, there is a lack of research on deriving the allometric growth scaling of multisource transportation networks.

In this paper, we propose a multisource transportation network (MTN) model by expanding on the STN model. Furthermore, we apply our model to predict the allometric growth exponents of river, freight and gasoline station systems. The results show that the MTN model can provide an alternative explanation of the origin of the allometric growth exponent in the range of $[D/(D+1), 1]$. This suggests that our model presents a new theoretical framework to explain the allometric growth phenomenon in both natural and social systems.

2. Multisource transportation network model

2.1. Single-source transportation network model

The basic rule of the STN model is that nutrients are transported from a central source to transfer sites through a resource transportation network [7], as shown in figure 1(a).
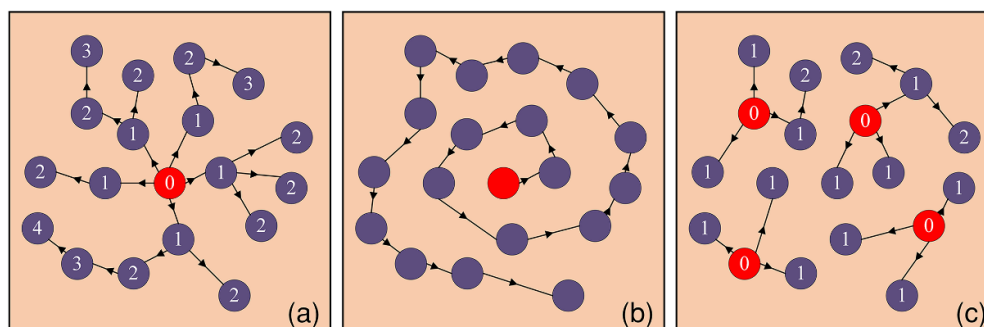
Figure 1. Single-source and multisource transportation networks. (a) Single-source transport network (directed spanning tree network). Each circle represents a transfer site. The number on the circle represents the distance from the transfer site to the central source, and the red point with a distance of 0 is the central source. (b) Single-source transport network (coiled network). (c) Multisource transportation network. The red points with a distance of 0 are the sources.

Transfer sites are points that accept and transfer nutrients in the network. When nutrients pass through a transfer site, a portion is absorbed by the site, while the remainder continues to be transported to the next layer, and so on, until reaching the final layer where there is no further outflow. The number of transfer sites is L^D, where L is a variable that represents the length of the organism, and is expressed in terms of the average distance between adjacent transfer sites. D is the Euclidean spatial dimension of the network. The total amount of nutrients transported to each site per unit time is $B \propto L^D$. In the case of steady-state supply, the structure of the transportation network determines the total blood volume C (proportional to the volume of the organism) of a given organism at any given time, and the most effective network is defined as the one with the smallest C. The relationship between C and network structure can be described as

$$C \propto L^D \langle L_X \rangle, \tag{1}$$

where $\langle L_X \rangle$ is the average distance of all transfer sites to the central source. We can attribute equation (1) to the fact that the network capacity (total blood volume C) must meet specific requirements, i.e. the transportation demand of all transfer sites can be met at once, to ensure a constant flow (metabolic volume B) is maintained in the transportation network. As a result, the network capacity is determined by multiplying the number of transfer sites (L^D) by the average distance ($\langle L_X \rangle$) between the transfer sites and the central source.

Banavar discovered that the directed spanning tree shown in figure 1(a) is the most efficient network, while the network shown in figure 1(b) is the least efficient. For these two networks, the values of $\langle L_X \rangle$ are L and L^D (see appendix for detailed derivation), respectively, from which the range of C can be obtained as follows:

$$L^{(D+1)} \leqslant C \leqslant L^{2D}. \tag{2}$$

As $B \propto L^D$, we can derive such a relationship between B and C when the network is the most efficient network:

$$B = C^{D/(D+1)}. \tag{3}$$

Equation (3) explains the allometric growth of three-dimensional organisms, two-dimensional rivers and even one-dimensional permeable tissue.

2.2. Multisource transportation network model

As mentioned above, Banavar tested the STN model in the river scenario and found that the allometric growth exponent of two-dimensional systems is 2/3. However, this model cannot capture the allometric growth phenomena in multisource networks. Depicting the impact of multiple sources on the allometric growth exponent is a significant challenge. For this problem, we first analyze the relationship between the total number of sources S and the network flow B. It is simple to determine that $S = f(B) = 1$ for a single-source network and $S = f(B) = B$ for a fully decentralized network. However, the $S = f(B)$ function for a multisource network is still obscure. Here we assume that there is a power-law relationship as $S \sim B^n$, where B is the flow for a general system. This assumption will be validated in subsequent empirical analyses (see section 3.1). At this point, the average distance $\langle L_X \rangle$ from all transfer sites to the source is no longer proportional to L because the number of sources becomes larger. The average number of transfer sites that are assigned to each source is $L^D/S = L^D/B^n = L^D/L^{D \cdot n} = L^{D-Dn}$. This leads to a relationship between $\langle L_X \rangle$ and L as

$$\langle L_X \rangle \sim \left(L^{D-Dn}\right)^{1/D} = L^{1-n}. \tag{4}$$

Substituting equation (4) into (1), we obtain

$$B = C^{D/(D+1-n)}. \tag{5}$$

Now we represent the influence of multiple sources on the allometric growth exponent and derive the equation for the allometric growth relation. The exponent $D/(D+1-n)$ depends on the Euclidean space dimension D of the network and the power exponent n between the number of sources and flows. When $n = 0$, the MTN model degenerates to the general STN network. When $n = 1$, the MTN model degenerates to the decentralized network [24].

2.3. Simulation

Now, we perform simulations on the multisource network to analyze the effect of n on the allometric growth exponent. For simplicity, we perform this work in a two-dimensional space. A multisource network implies that the nodes are divided into multiple sources to form their respective networks. We simulate such a network by the following steps.

(i) Add a number of randomly located points proportional to the spatial area L^2. As the transportation demand B is proportional to L^2 in two-dimensional space, the
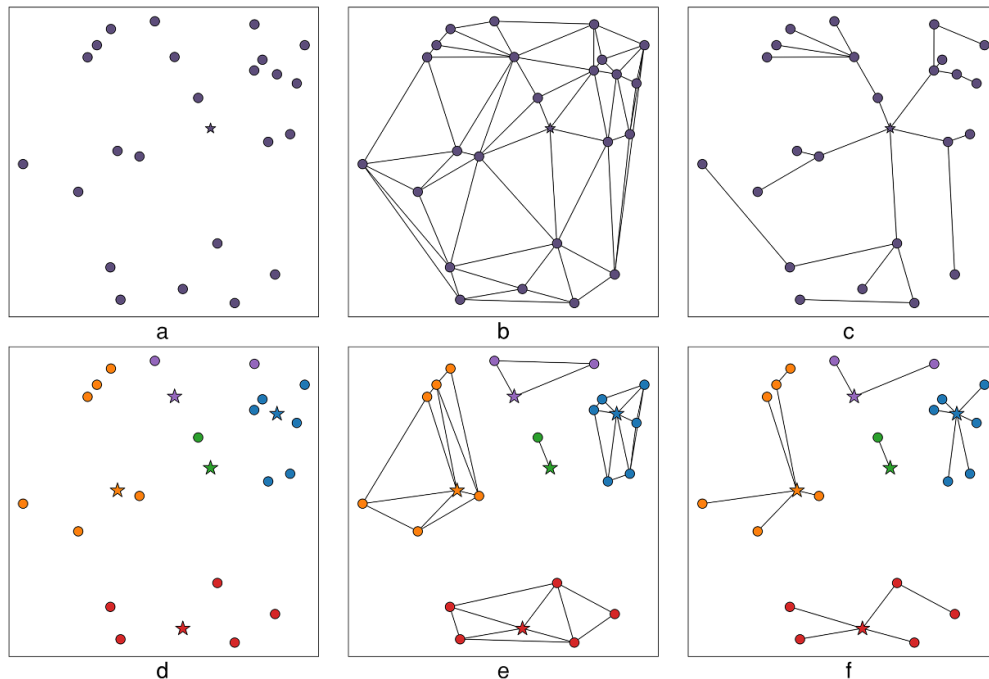
Figure 2. Method for generating the most efficient transportation network ($B = 25$), where (a)–(c) is the generation process of a single-source network ($n = 0$), and (d)–(f) is the generation process of a multisource network ($0 < n \leqslant 1$). (a) Add 25 points randomly in the two-dimensional space. For $n = 0$, the number of clusters is $B^n = 25^0 = 1$. The pentagram point is the central point. (b) Connect all points into a connected single-source network using the Delaunay triangle algorithm. (c) Generate a breadth-first spanning tree of this connected network, which is the most efficient network. (d) In the case of $n = 0.5$, the number of clusters is $B^n = 25^{0.5} = 5$. Aggregate the points generated in (a) into five clusters by the K-means space clustering algorithm, where points of the same color belong to the same cluster and the pentagram point is the central point of the cluster. (e) Connect all nodes of each cluster separately into a connected subgraph using the Delaunay triangle algorithm. (f) Generate a breadth-first spanning tree for each subgraph.

number of points is also proportional to B. An example with 25 points ($B = 25$) is shown in figure 2(a).

(ii) Given the number of sources of B^n, the points generated in the previous step are divided into B^n clusters by the K-means space clustering algorithm, and the point closest to the clustering center is regarded as the source of each cluster. Figures 2(a) and (d) show different scenarios for $n = 0$ and $n = 0.5$, respectively.

(iii) Connect all points of each cluster into a connected subgraph using the Delaunay triangle algorithm (see figures 2(b) and (e)).

(iv) Generate a breadth-first spanning tree (BFST) from the source point in each subgraph, as shown in figures 2(c) and (f). The resulting BFST network is the most efficient transportation network [7].
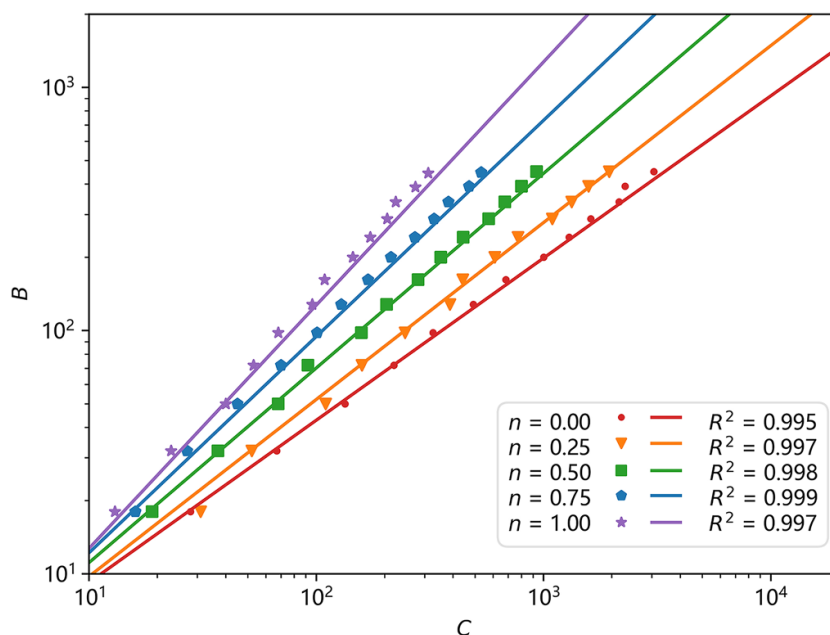
Figure 3. Simulation results. The horizontal axis (C) and vertical axis (B) represent the capacity of the transportation network and the transportation demand of the network sites, respectively. n is the power exponent between the number of sources and the transportation demand. Each point represents the simulation result of C when n and B take different values. The straight lines are the theoretical results of the MTN model. The slope of the straight line is the theoretical value of the $B - C$ allometric growth exponent calculated by the MTN model. R^2 is the coefficient of determination between the simulation results and the theoretical results.

(v) Calculate the network capacity C for each BFST network by computing the sum of the network distances (the shortest number of edges) of all nodes to the source of the BFST network.

(vi) Sum the network capacity C of each BFST network to calculate the C of the entire multisource network.

According to the above algorithm, we can obtain different values of C by setting different values of n and B. C in practical measurement serves as a metric for evaluating network capacity, such as the blood volume in a metabolic system or the watershed area in a river system. Figure 3 shows the comparison between the simulation results and the theoretical allometric growth line. The points and line show the simulated and theoretical relationships between B and C, respectively, when n takes a definite value. The simulation results are quite close to the theoretical results. As n increases, the allometric growth exponent also increases according to the pattern in equation (5).

3. Application of the MTN model

In this section, we apply the MTN model to analyze the allometric growth of Chinese river, Chinese freight and U.S. gasoline station systems.

3.1. Application to Chinese river system

Our first application of the MTN model is in the Chinese river system. We gather and examine data for some rivers that are part of the Taizi River system in China (see figure 4(a)). From these data, we can determine an allometric growth relationship between the annual runoff, defined as the total amount of water that flows out of the river network over the course of a year (network flow B), and the watershed area, which is the geographical area in which all the water drains into the river system (network capacity C). We use the least squares regression method (which is also used for subsequent exponents estimation) on the Taizi River system data to estimate the allometric growth exponent, resulting in a scaling exponent of 0.654 (very close to 2/3), as shown in figure 4(b) and table 1. However, the exponent becomes 0.905 (see figure 4(c) and table 1) when we examine the relationship between annual runoff and watershed area for river systems (consisting of mainstream and its tributaries, see figure 4(a)). This is because the river system is a multisource transportation network, with the confluences of the mainstream and tributaries serving as the sources [25]. By counting the relationship between the number of sources S and annual runoff B in the river system networks (as shown in figure 4(d)), we find an approximate power-law relationship as $S \sim B^{0.726}$. Substituting the power-law exponent n between S and B into equation (5), we can obtain $B = C^{0.882}$, which covers the exponent 0.905 in figure 4(c) (see table 1). Thus, it is clear that the MST model is an alternative tool that can be used for analyzing the allometric growth relationship of the river system.

3.2. Application to the Chinese freight system

We begin by constructing a freight transportation network using Chinese freight data (related to trucks) [26]. We first extract the travel trajectories of each truck within the city from our basic truck data. For each long-time parking point in the travel trajectory, we consider the enterprise closest to it as a loading and unloading enterprise [26]. The enterprise with the most appearances in each travel trajectory is considered the travel trajectory source, and multiple travel trajectories with the same source are combined as a freight source. In this freight network, the number of network sources S can be represented by the number of freight sources, the transportation demand B can be represented by the number of trucks in a city, and network capacity C can be represented by the urban population. We then count the relationship between the freight sources and the number of city trucks as $S \sim B^{0.960}$ (see figure 5(a)). Substituting n into equation (5), we obtain $B = C^{0.980}$ (see table 1). We then count the actual allometric growth relationship between the number of urban trucks and the urban population, as shown in figure 5(b). The actual data show that $B \sim C^{0.950}$. The allometric growth exponent calculated with the MTN is within the deviation range of the actual data
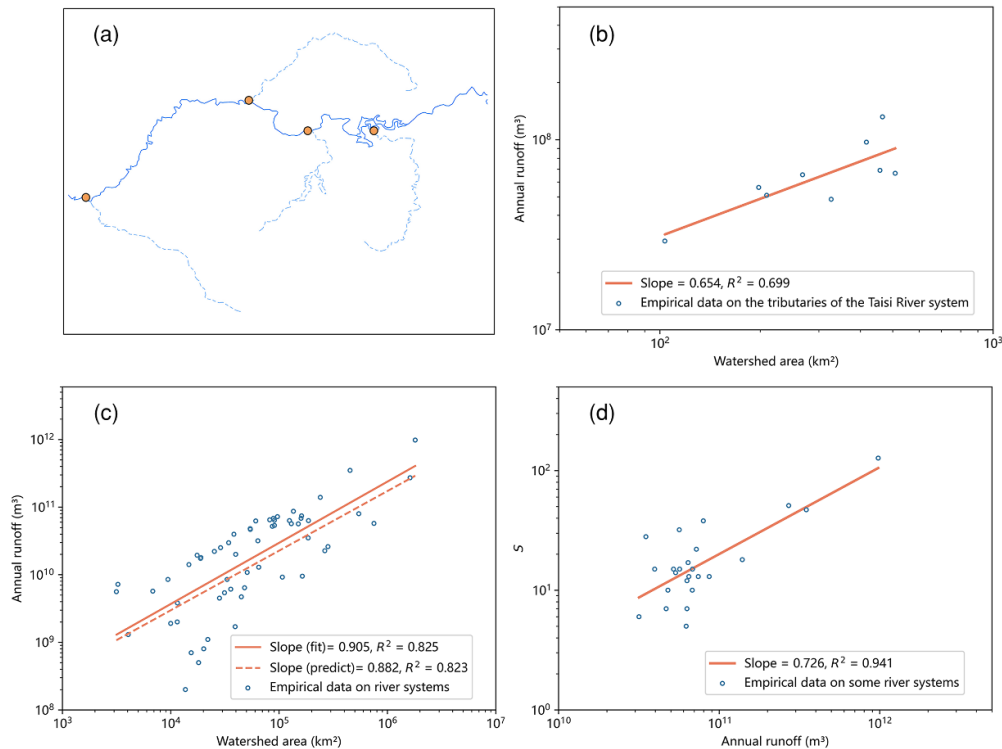
Figure 4. Relationship between the annual runoff and watershed area for some river systems and some rivers within the Chinese Taizi River system. (a) Schematic diagram of the mainstem and tributaries of the Taizi River (partial). The solid curve is the main stream, the dotted curve is the tributary, and the nodes are the confluence of the main and tributary streams. (b) Relationship between the annual runoff and watershed area of some tributaries within the Taizi River system. The slope of the fitted line is 0.654 ($R^2 = 0.699$). (c) Relationship between the annual runoff and watershed area of major river systems in China. The slope of the fitted line (solid line) is 0.905 ($R^2 = 0.825$), and the slope of the predicted line(dotted line) is 0.882 ($R^2 = 0.823$). (d) Relationship between the number of central sources and the annual runoff of the river system network. The slope of the fitted line is 0.726 ($R^2 = 0.941$).

calculation results (see table 1), which suggests that the MTN model captures the essence of the allometric growth of freight systems.

3.3. Application to the U.S. gasoline sales system

The gasoline distribution network is a multisource network, similar to the freight network. We can use the number of gas stations to represent the number of sources S in the network, the quantity of gasoline sales to represent the transportation demand B of the network [27], and the urban population to indicate the network capacity C. We count the relationship between S and B, as shown in figure 6(a), which gives $S \sim B^{0.787}$. We can obtain $B = C^{0.904}$ by using the MTN model. We then count the relationship between urban gasoline sales and the urban population, as shown in figure 6(b), and obtain $B = C^{0.841}$. The calculation results of the MTN model are close to the statistical
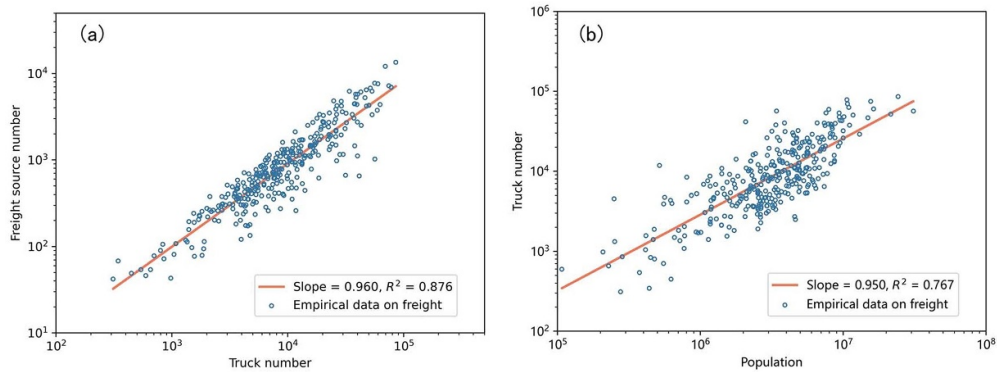
Figure 5. Empirical data on the allometric growth of the Chinese urban freight system. (a) Relationship between the number of freight sources and urban trucks. The slope of the fitted line is 0.960 ($R^2 = 0.876$). (b) Relationship between the number of urban trucks and urban population. The slope of the fitted line is 0.950 ($R^2 = 0.767$).

Table 1. Empirical and model allometric growth exponents in different systems.

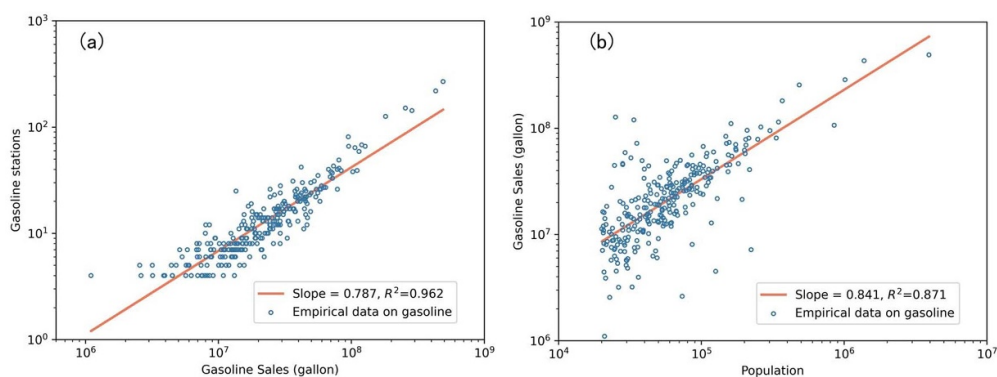| System	Empirical exponent	R^2	Standard deviation	Model exponent	Relative error (%) between empirical and model exponents
Tributaries	0.654	0.699	±0.181	0.667	1.99
River systems	0.905	0.825	±0.107	0.882	2.54
Trucks	0.950	0.767	±0.039	0.980	3.16
Gas stations	0.841	0.871	±0.047	0.904	7.49

Figure 6. Empirical data of the allometric growth of U.S. gasoline sales system. (a) Relationship between the number of gas stations and gasoline sales. The slope of the fitted line is 0.787 ($R^2 = 0.962$). (b) Relationship between gasoline sales and population. The slope of the fitted line is 0.841 ($R^2 = 0.871$).

results of the actual data (see table 1), which further demonstrates the applicability of the MTN model.

4. Conclusion and discussion

Allometric growth is pervasive and has a considerable research significance in both natural and social systems [28–31]. Banavar *et al* discovered that a single-source transportation network with maximum efficiency is where the allometric growth exponent $D/(D+1)$ emerges [7, 32]. However, their work was unable to reproduce the diversified allometric growth exponents [9, 33, 34]. In response to this problem, we conduct an empirical study of river systems and find that the allometric growth exponent depends on the number of sources in the transportation network. Based on the results, we propose an MTN model that can describe allometric growth with an exponent in the range of $[D/(D+1),1]$ for single-source and multisource networks. We apply the MTN model to sufficiently reproduce the allometric growth exponents of not only river but also freight and gas station systems, indicating that our model is generalizable.

Empirical studies have found that the exponent of multisource urban systems usually ranges from 0.7 to 0.9 [9]. The MTN model suggests that an increase in the number of sources leads to an increase in efficiency (and the exponent). However, it remains a question as to why the number of sources in real-world systems does not reach the maximum, resulting in an exponent that does not reach the theoretical maximum of 1. One possible explanation for this phenomenon is that cities must balance efficiency and cost [35–39]. As the number of sources increases, the cost of implementing the system also increases [40], forcing urban systems to make trade-offs. Although we have reproduced and explained the diversity urban allometric growth exponent, we do not yet know the process by which the urban system reaches an efficiency-cost equilibrium. Therefore, the mechanism of efficiency-cost equilibrium in urban systems deserves further study.

It's important to note that the data sets we used in this paper have some limitations, particularly their discrete nature. For instance, the empirical result of the truck number versus population has an R^2 value lower than 0.8. Future work could benefit from employing higher quality and more comprehensive data sets to further validate and refine our model. Furthermore, while our model can explain allometric growth exponents in the range of $[D/(D+1),1]$, it currently does not account for systems with allometric growth exponent exceeding 1. Although our model can derive $Y \sim C^{((D+2-2n)/(D+1-n))}$ with allometric growth exponent in the range of $[1,(D+2)/(D+1)]$ by combining Bettencourt's hypothesis [35] that socioeconomic output Y is equal to the product of the urban population C and the per capita interaction C/B, this hypothesis still needs to be verified in non-urban systems. Future research should focus on extending our model or developing new ones to capture phenomena across all allometric growth exponents [9, 19].
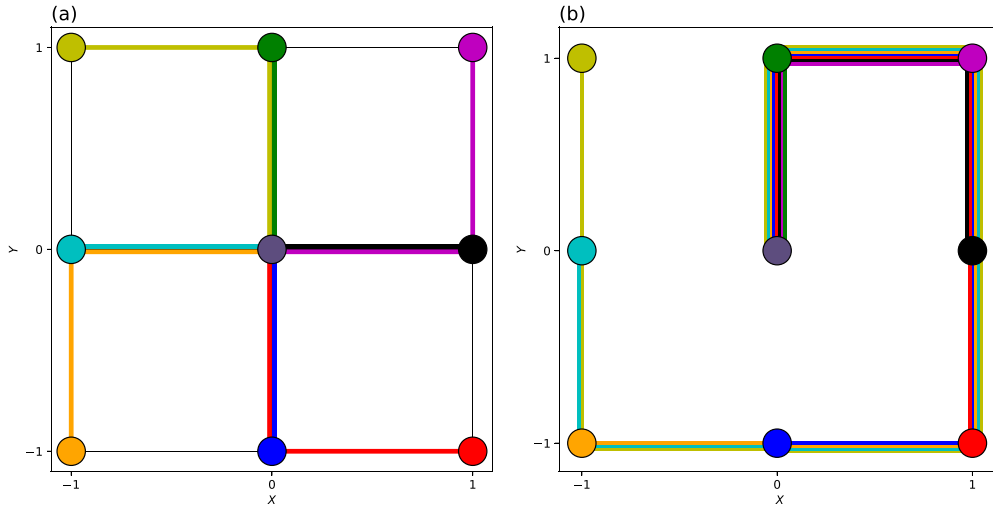
Figure A1. Schematics of the most efficient network (a) and the least efficient network (b) within a two-dimensional grid scenario. Both grids encompass a side length of 3, uniformly distributing 9 nodes with the central node situated at (0,0). Paths from the central point to distinct nodes are identified by lines of the node's color. In the most efficient network (a), the Manhattan distance from any given node to the center amounts to the sum of the absolute values of the node's x and y coordinates. Conversely, in the least efficient network (b), each node is connected to the center via a spiral path.

Appendix

In this appendix, we derive the expressions for $\langle L_X \rangle$ associated with the most efficient and least efficient networks. We begin with a discussion in the context of two-dimensional space.

The most efficient network is visualized as a two-dimensional grid, featuring a side length of L and consisting of L^2 nodes, as shown in figure A1(a). We locate the center node at the coordinate origin (0,0) and compute the Manhattan distance for each node from the center. Nodes have integer coordinates, spanning from $-\frac{(L-1)}{2}$ to $\frac{(L-1)}{2}$ (assuming L to be an odd number for the purpose of defining a distinct center). The distance is the sum of the absolute values of the x and y coordinates for each node. With each distinct x or y coordinate, there are L nodes spanning the entire grid along the other axis. Hence, the total absolute value of x coordinates of all nodes is $2 \times \sum_{i=0}^{(L-1)/2} i \times L$ (the same applies to y coordinates). Accordingly, the average distance from all nodes to the center can be computed as

$$\langle L_X \rangle = \frac{1}{L^2} \times 4 \times \sum_{i=0}^{(L-1)/2} i \times L = \frac{L}{2} - \frac{1}{2L} \approx \frac{L}{2} \sim L. \tag{A.1}$$

In contrast, the least efficient network, as visualized in figure A1(b) and as hypothesized by Banavar *et al* [7], resembles a spiral where each node is exclusively connected to

its adjacent neighbors. Here, the distance from the center node to the ith node equals i. Therefore, the average distance can be estimated as the sum from 1 to L^2, divided by the total node count (L^2), giving

$$\langle L_X \rangle = \frac{1}{L^2} \times \sum_{i=0}^{L^2} i = \frac{1}{L^2} \times \frac{L^2 \times (L^2 + 1)}{2} = \frac{(L^2 + 1)}{2} \sim L^2. \tag{A.2}$$

The above explanation highlights the characteristics of the most and least efficient networks in terms of $\langle L_X \rangle$. Specifically, $\langle L_X \rangle$ grows linearly with L in the most efficient network, while it expands in the order of L^D in the least efficient network.

References

[1] Kleiber M 1947 Body size and metabolic rate *Physiol. Rev.* **27** 511–41
[2] West G B, Brown J H and Enquist B J 1997 A general model for the origin of allometric scaling laws in biology *Science* **276** 122–6
[3] Damuth J 2001 Scaling of growth: plants and animals are not so different *Proc. Natl Acad. Sci. USA* **98** 2113–4
[4] White C R, Alton L A, Bywater C L, Lombardi E J and Marshall D J 2022 Metabolic scaling is the product of life-history optimization *Science* **377** 834–9
[5] De Martino S and De Siena S 2012 Allometry and growth: a unified view *Physica* A **391** 4302–7
[6] Dreyer O 2001 Allometric scaling and central source systems *Phys. Rev. Lett.* **87** 038101
[7] Banavar J R, Maritan A and Rinaldo A 1999 Size and form in efficient transportation networks *Nature* **399** 130–2
[8] Lee Y 1989 An allometric analysis of the us urban system: 1960–80 *Environ. Plan.* A **21** 463–76
[9] Bettencourt L M A, Lobo J, Helbing D, Kühnert C and West G B 2007 Growth, innovation, scaling and the pace of life in cities *Proc. Natl Acad. Sci. USA* **104** 7301–6
[10] West G 2018 *Scale: The Universal Laws of Life, Growth and Death in Organisms, Cities and Companies* (Penguin)
[11] Arbabi H, Mayfield M and McCann P 2020 Productivity, infrastructure and urban density—an allometric comparison of three european city regions across scales *J. R. Stat. Soc.* A **183** 211–28
[12] Yakubo K, Saijo Y and Korošak D 2014 Superlinear and sublinear urban scaling in geographical networks modeling cities *Phys. Rev.* E **90** 022803
[13] Horta-Bernús R, Rosas-Casals M and Valverde S 2010 Discerning electricity consumption patterns from urban allometric scaling *2010 Complexity in Engineering* (IEEE) pp 49–51
[14] Zhang J and Tongkui Y 2010 Allometric scaling of countries *Physica* A **389** 4887–96
[15] Oliveira E A, Andrade J S and Makse H A 2014 Large cities are less green *Sci. Rep.* **4** 4235
[16] Zhao S, Liu S, Chunxue X, Yuan W, Sun Y, Yan W, Zhao M, Henebry G M and Fang J 2018 Contemporary evolution and scaling of 32 major cities in China *Ecol. Appl.* **28** 1655–68
[17] Dong H, Menghui Li, Liu R, Chensheng W and Jinshan W 2017 Allometric scaling in scientific fields *Scientometrics* **112** 583–94
[18] Cempel C, Tabaszewski M and Ordysiński S 2016 Allometric scaling and accidents at work *Int. J. Occup. Saf. Ergon.* **22** 173–8
[19] Rocha L E C, Ryckebusch J, Schoors K and Smith M 2021 The scaling of social interactions across animal species *Sci. Rep.* **11** 12584
[20] Han W and Fang J 2008 Review on the mechanism models of allometric scaling laws: 3/4 vs. 2/3 power *Chin. J. Plant Ecol.* **32** 951
[21] Roy Frieden B and Gatenby R A 2005 Power laws of complex systems from extreme physical information *Phys. Rev.* E **72** 036101
[22] Zhang J, Liu Y, Zhao Y and Deng T 2020 Emergency evacuation problem for a multi-source and multi-destination transportation network: mathematical model and case study *Ann. Oper. Res.* **291** 1153–81
[23] Yassin-Kassab A, Templeman A B and Tanyimboh T T 1999 Calculating maximum entropy flows in multi-source, multi-demand networks *Eng. Optim.* **31** 695–729
[24] Samaniego H and Moses M E 2008 Cities as organisms: allometric scaling of urban road networks *J. Transp. Land Use* **1** 21–39

[25] Roy A, Rhoads B and Rice S 2008 *River Confluences, Tributaries and the Fluvial Network* (Wiley)
[26] Yang Y, Jia B, Yan X-Y, Jiangtao Li, Yang Z and Gao Z 2022 Identifying intercity freight trip ends of heavy trucks from GPS data *Transp. Res.* E **157** 102590
[27] California Energy Commission. California retail fuel outlet annual reporting 2021 (available at: www.energy.ca.gov/data-reports/energy-almanac/transportation-energy/california-retail-fuel-outlet-annual-reporting)
[28] Chen Y 2017 Multi-scaling allometric analysis for urban and regional development *Physica* A **465** 673–89
[29] Chen Y, Wang Y and Xijing Li 2019 Fractal dimensions derived from spatial allometric scaling of urban form *Chaos, Solitons Fractals* **126** 122–34
[30] Salingaros N A and West B J 1999 A universal rule for the distribution of sizes *Environ. Plan.* B **26** 909–23
[31] Lan T, Peng Q, Wang H, Gong X, Jing Li and Shi Z 2021 Exploring allometric scaling relations between fractal dimensions of metro networks and economic, environmental and social indicators: a case study of 26 cities in China *ISPRS Int. J. Geo-Inf.* **10** 429
[32] Sheridan Dodds P 2010 Optimal form of branching supply and collection networks *Phys. Rev. Lett.* **104** 048702
[33] Glazier D S 2005 Beyond the '3/4-power law': variation in the intra-and interspecific scaling of metabolic rate in animals *Biol. Rev.* **80** 611–62
[34] Savage V M, Deeds E J and Fontana W 2008 Sizing up allometric scaling theory *PLoS Comput. Biol.* **4** e1000171
[35] Bettencourt L M A 2013 The origins of scaling in cities *Science* **340** 1438–41
[36] Warner M E and Hefetz A 2008 Managing markets for public service: the role of mixed public–private delivery of city services *Public Adm. Rev.* **68** 155–66
[37] Tero A, Takagi S, Saigusa T, Ito K, Bebber D P, Fricker M D, Yumiki K, Kobayashi R and Nakagaki T 2010 Rules for biologically inspired adaptive network design *Science* **327** 439–42
[38] Mimar S, Soriano-Paños D, Kirkley A, Barbosa H, Sadilek A, Arenas A, Gómez-Gardeñes J and Ghoshal G 2022 Connecting intercity mobility with urban welfare *PNAS Nexus* **1** pgac178
[39] Naphade M, Banavar G, Harrison C, Paraszczak J and Morris R 2011 Smarter cities and their innovation challenges *Computer* **44** 32–39
[40] Gudehus T and Kotzab H 2012 *Comprehensive Logistics* (Springer)